



JOURNAL OF
APPLIED
CRYSTALLOGRAPHY

Volume 52 (2019)

Supporting information for article:

Investigating temperature-induced structural changes of lead halide perovskites by *in situ* X-ray powder diffraction

Rocco Caliandro, Davide Altamura, Benny Danilo Belviso, Aurora Rizzo, Sofia Masi and Cinzia Giannini

SUPPLEMENTARY INFORMATION

Investigating temperature-induced structural changes of lead halide perovskites by in situ X-ray powder diffraction

Rocco Caliendo, Davide Altamura, Benny Danilo Belviso, Aurora Rizzo, Sofia Masi
and Cinzia Giannini

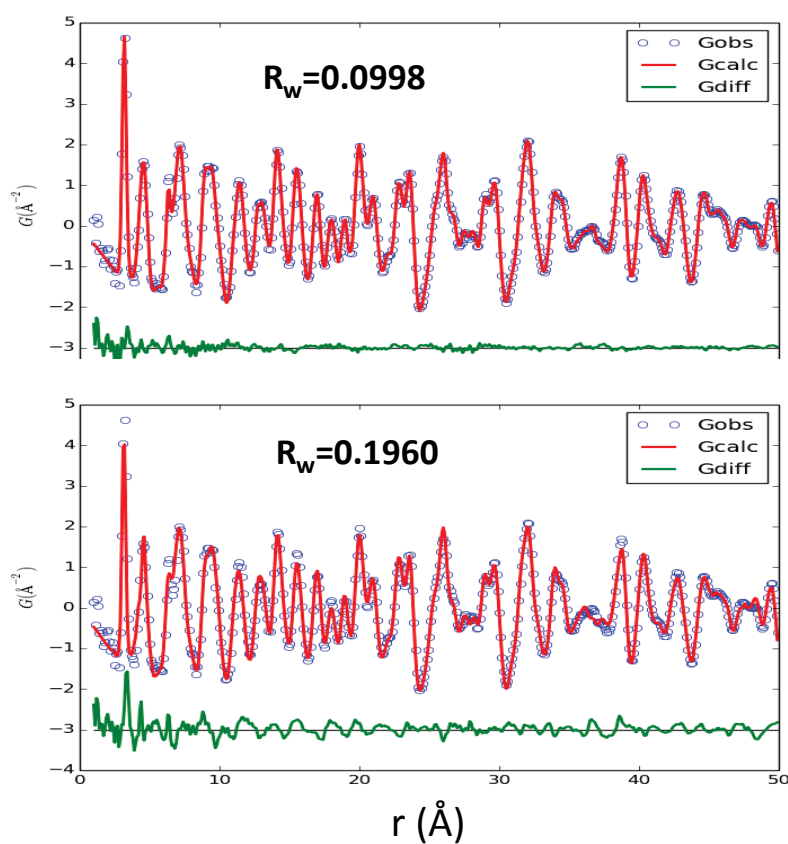


Figure S1. Experimental pair distribution function of sample Pero2 at 300 K (open circles), fitted by using the tetragonal (top) and cubic (bottom) crystal structure of MAPbI_3 (red lines), in addition to the PbI_2 -MAI-DMSO crystal model. The difference between experimental and fitted model (green line) and the values of the weighted agreement factor between the two profiles R_w are shown.

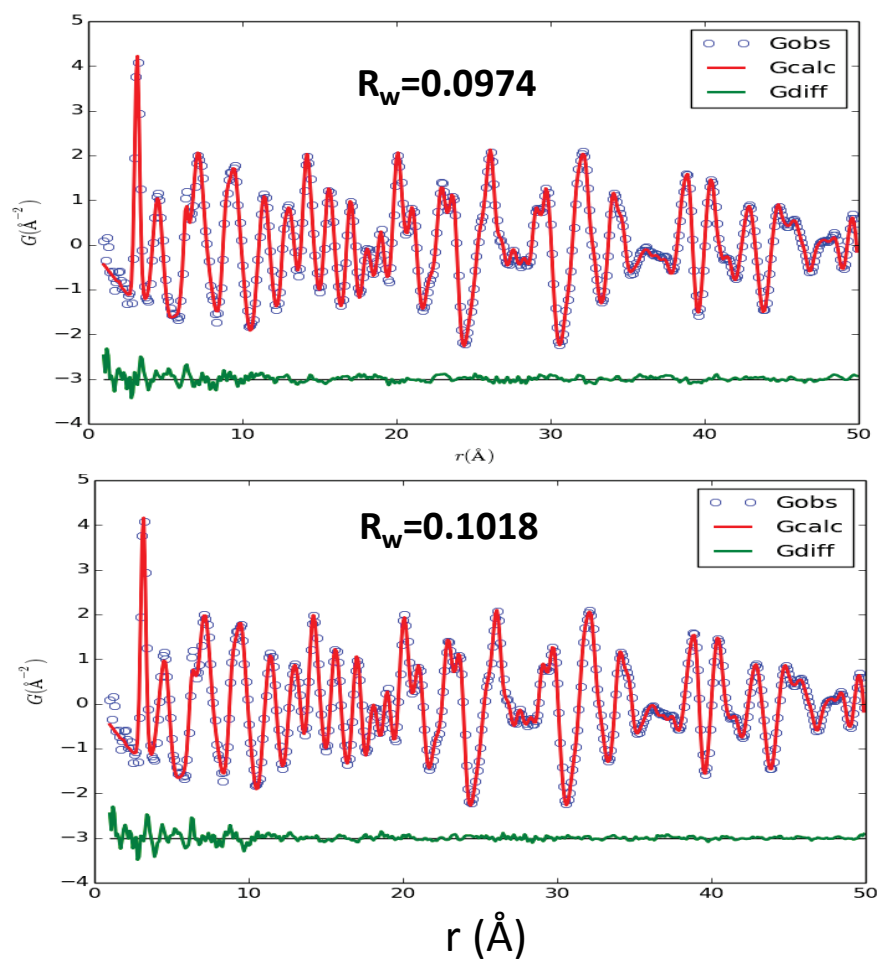


Figure S2. Experimental pair distribution function of Pero2 sample at 400 K (open circles), fitted by using the tetragonal (top) and cubic (bottom) crystal structure of MAPbI₃ (red lines), in addition to the PbI₂-MAI-DMSO crystal model. The difference between experimental and fitted model (green line) and the values of the weighted agreement factor between the two profiles R_w are shown.

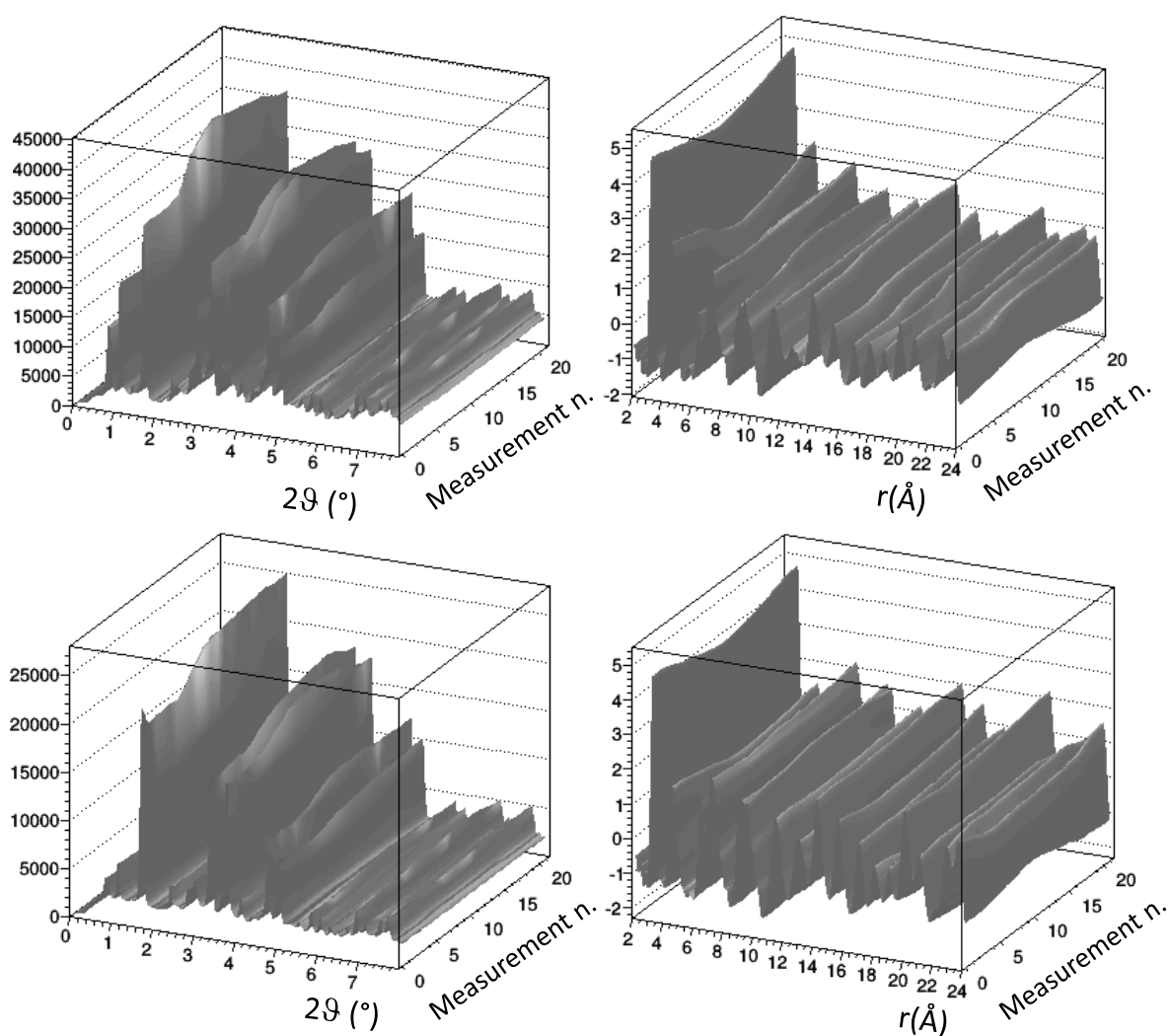


Figure S3. X-ray powder diffraction (left) and pair distribution function (right) data matrices obtained for Pero1 (top) and Pero2 (bottom) samples from the *in situ* experiment, shown in surface representation. Profiles are here truncated to highlight differences, but they have been measured up to $2\theta=40^\circ$ and calculated up to $r=50 \text{ \AA}$.

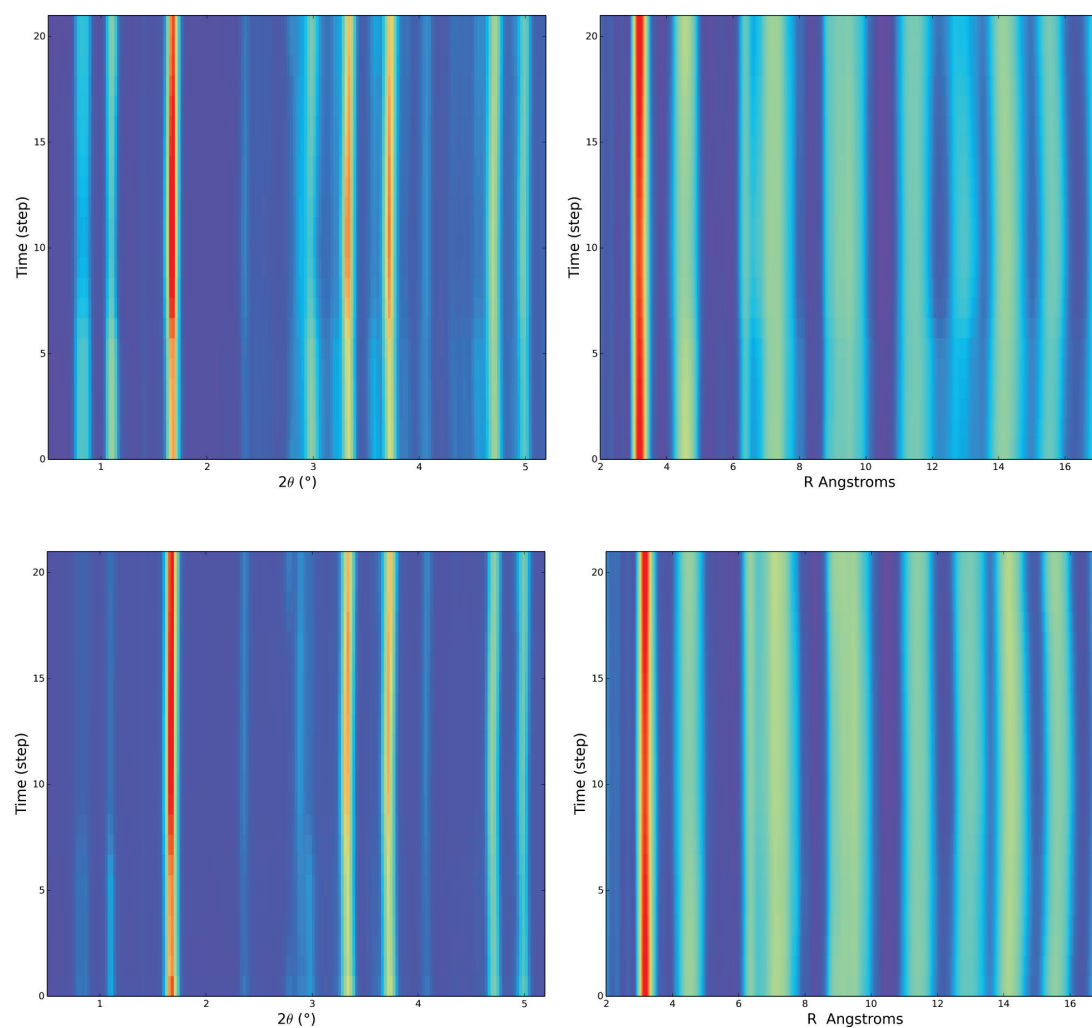


Figure S4. Top view of X-ray powder diffraction (left) and pair distribution function (right) data matrices obtained for Pero1 (top) and Pero2 (bottom) samples from the *in situ* experiment.

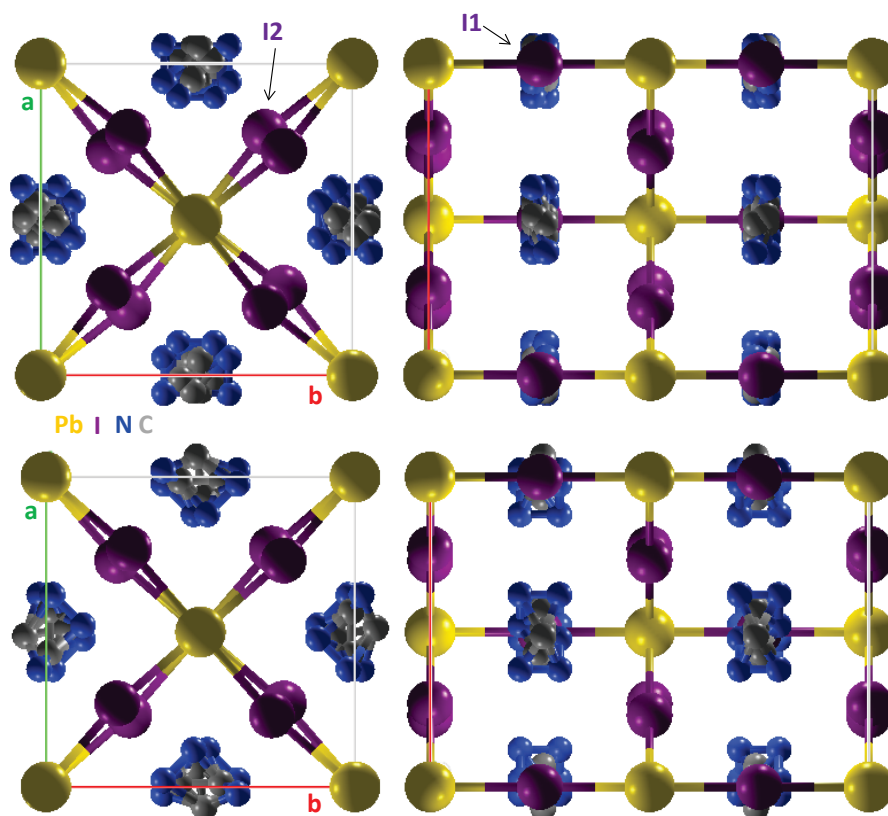


Figure S5. MAPbI₃ tetragonal crystal phase best fitted against XRPD data at T=300 K (top) and T=400 K (bottom) for Pero1 sample. Views in the (ab) plane (left) and in the (bc) plane (right). Colouring code is yellow for Pb, pink for I, blue for N and grey for C. I atoms on the (ab) plane are named I2, those aligned to Pb atoms along c are named I1.

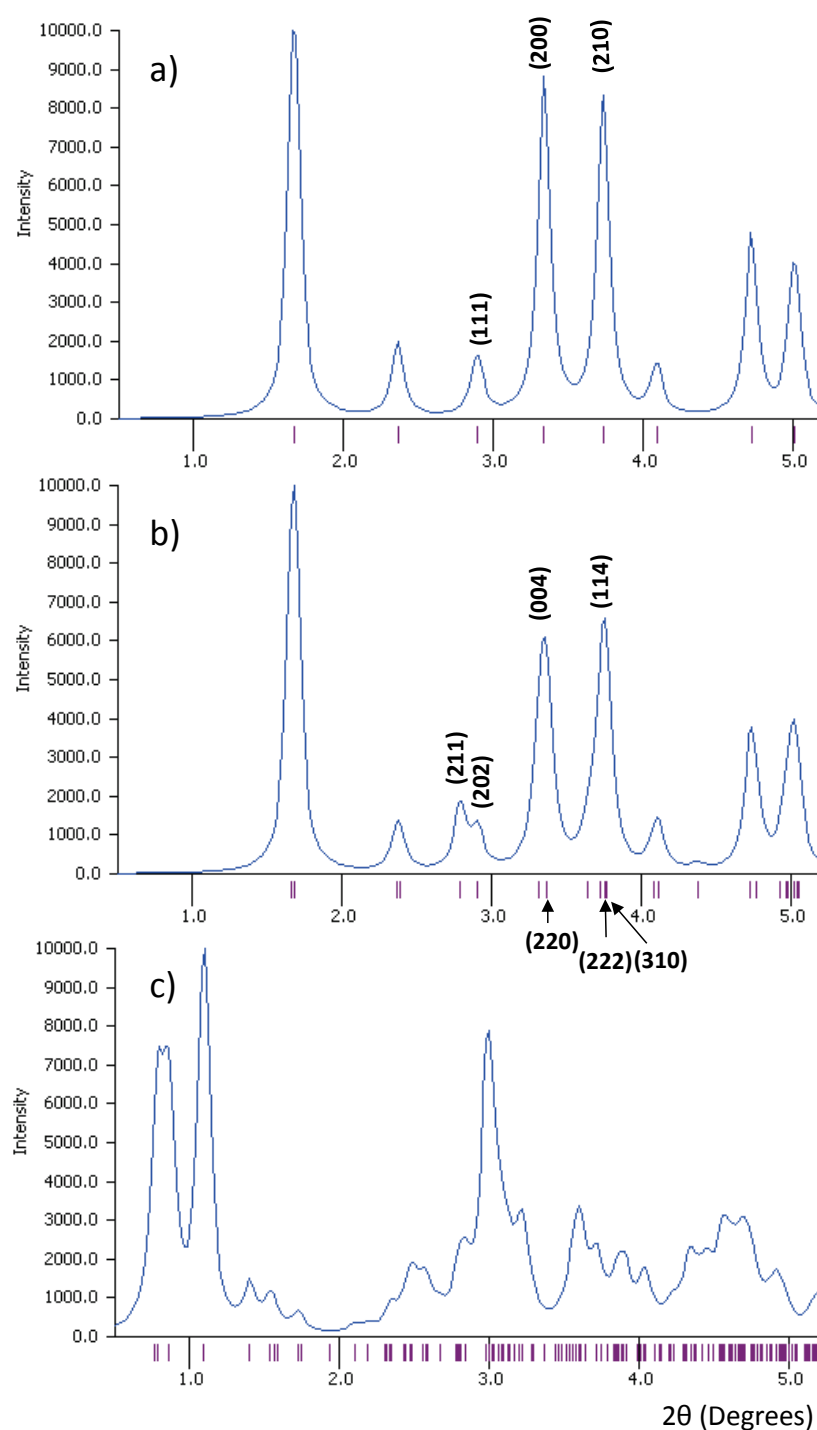


Figure S6. Powder diffraction patterns generated at a wavelength of 0.18372 \AA from known crystal structures of the cubic (a) and tetragonal (b) MAPbI_3 and the $\text{MAPbI}_2\text{-DMSO}$ (c). The reference patterns are reported on the 2θ axis. Purple bars indicate the position of expected reflections; relevant reflections discussed in the text are labelled. The peak at $2\theta = 2.8^\circ$ in (b), corresponding to reflection (211), is characteristic of the MAPbI_3 tetragonal phase and represents the R-point (311) superlattice Bragg reflection.

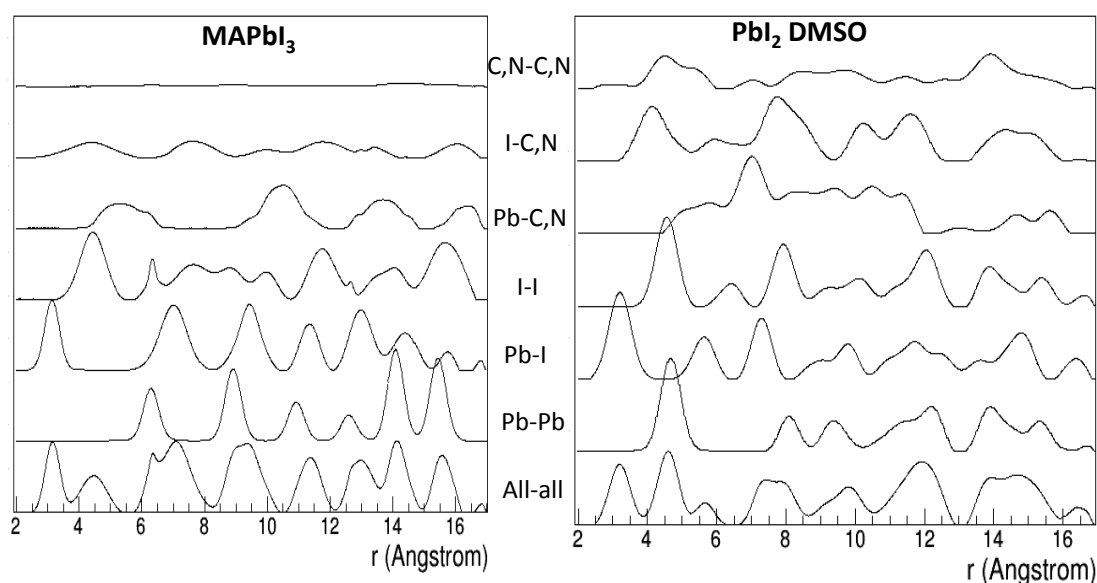


Figure S7. Contributions to pair distribution function calculated from the fitting model of the tetragonal MAPbI₃ (left) and orthorhombic PbI₂-MAI-DMSO (right) crystal structures fitted to the Pero1 sample. Atom types of pairs considered for each contribution are reported in the centre. All-all corresponds to all interatomic distances, thus coincides with the fitted PDF. Contributions are rescaled to have the same mean and the same variance.

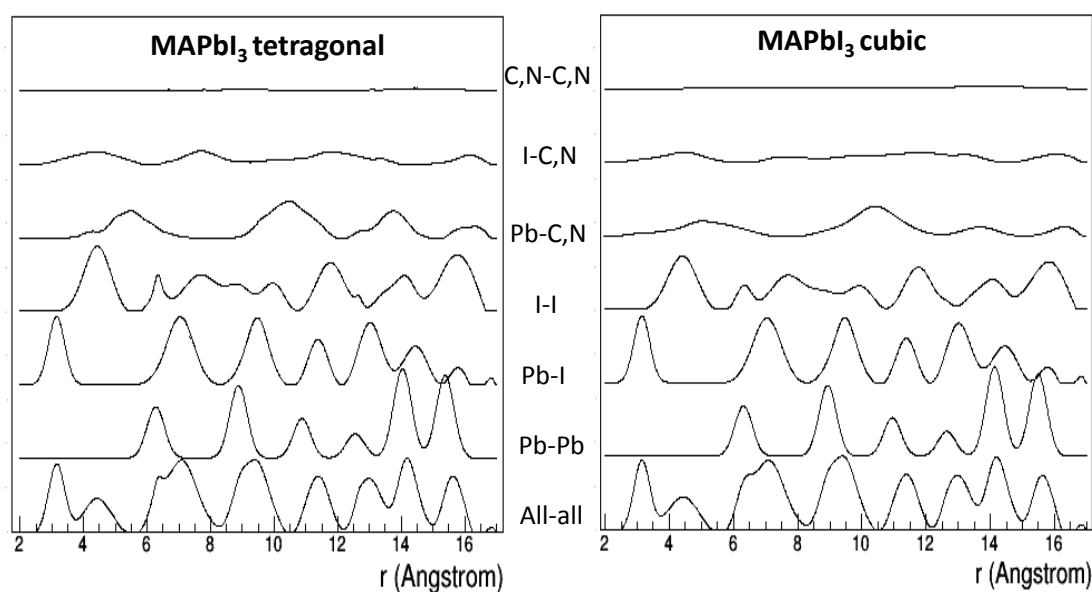


Figure S8. Contributions to pair distribution function calculated from the fitting model of the tetragonal (left) and cubic (right) MAPbI₃ crystal structures fitted to the Pero2 sample. Atom types of pairs considered for each contribution are reported in the centre. All-all corresponds to all interatomic distances, thus coincides with the fitted PDF. Contributions are rescaled to have the same mean and the same variance.

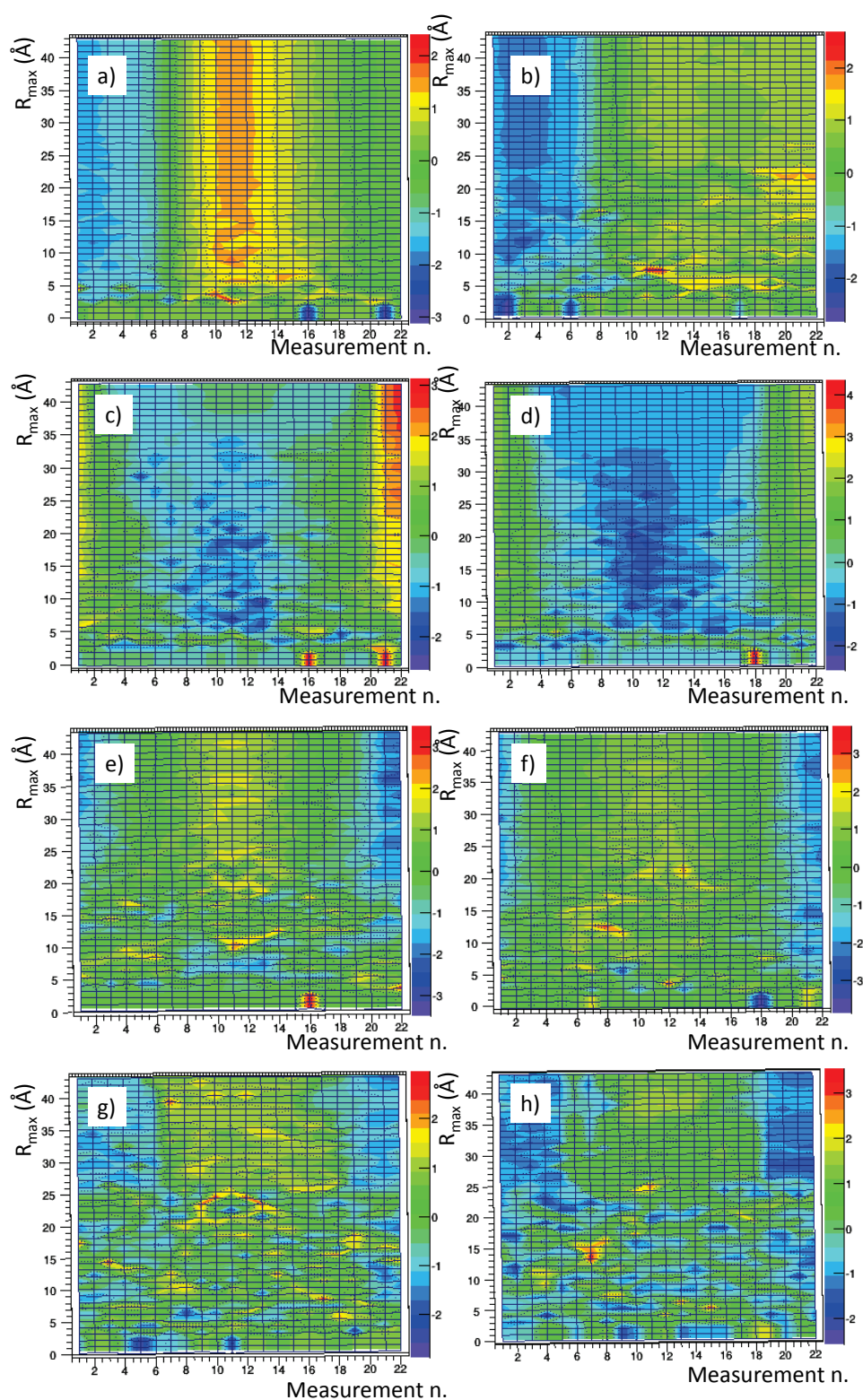


Figure S9. Structural parameters of the MAPbI_3 crystal phase of Pero1 (left) and Pero2 (right) samples determined by fitting the PDF profiles, plotted as a function of the maximum interatomic distance chosen for the PDF fitting (R_{max}). Weight fraction (a,b), dihedral angle I2-Pb-Pb-I2 (c,d), cell parameter a (e,f), methylammonium shape parameter (g,h).

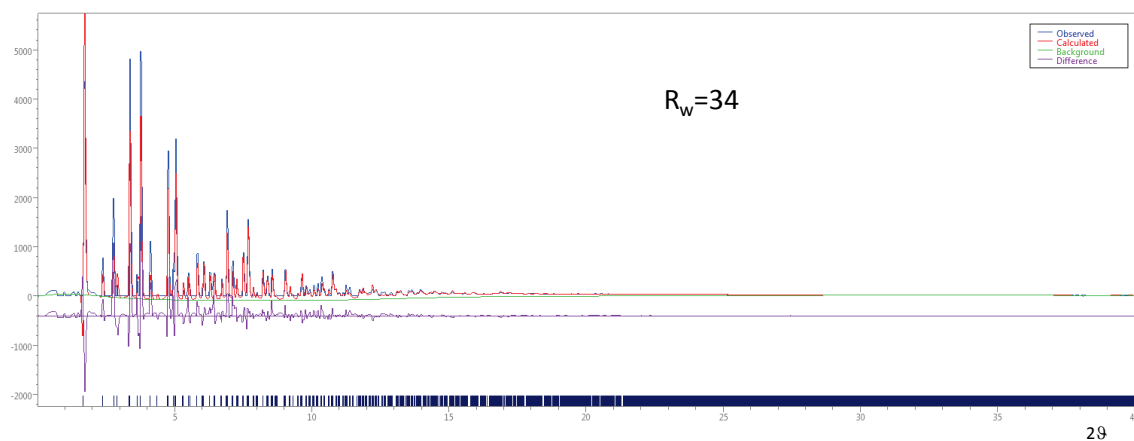


Figure S10. Results of Rietveld analysis applied to a profile obtained from principal component analysis applied to the Pero2 sample. PC1 loadings processed by putting at zero negative values have been used as observed profile (blue line). Profile calculated from the refined crystal structure (red line), estimated background (green line) and difference between observed and calculated profiles (violet line) are shown. The value of the weighted profile agreement factor (R_w) is reported.